Physica A 559 (2020) 125023

Contents lists available at ScienceDirect

Physica A

journal homepage: www.elsevier.com/locate/physa

A novel lattice hydrodynamic model accounting for driver's memory effect and the difference of optimal velocity on curved road

Qingying Wang, Rongjun Cheng, Hongxia Ge *

Faculty of Maritime and Transportation, Ningbo University, Ningbo 315211, China
Jiangsu Province Collaborative Innovation Center for Modern Urban Traffic Technologies, Nanjing 210096, China
National Traffic Management Engineering and Technology Research Centre Ningbo University Sub-centre, Ningbo 315211, China

ARTICLE INFO

Article history:
Received 2 October 2019
Received in revised form 14 May 2020
Available online 8 August 2020

Keywords:
Traffic flow
Lattice hydrodynamic
Curved road
Driver's memory effect
The difference of optimal velocity

ABSTRACT

A novel lattice hydrodynamic model is put forward, which takes the effects of driver's memory and difference of optimal velocity into account on curved road. Linear stability analysis for the novel model is discussed and the stability condition is deduced. Through nonlinear analysis, the mKdV equation is deduced to explore the evolution of jams near the vertex. The exact solution of the mKdV equation is also derived. The influence of the above two factors on traffic stability are investigated by numerical examples. Both numerical and analytical results demonstrate that memory effect and the difference of optimal velocity on curved road can ease traffic jams efficiently.

1. Introduction

In our modern society, traffic congestion is a serious problem which affects our daily life. As traffic jams become more and more serious, this phenomenon has attached the attention of a large number of scholars and researchers, and corresponding solutions of the problem are presented. In fact, the traffic environment is diversified and constantly changing, so a series of traffic models [1–38] have been proposed continuously, which include the cellular automation models [1–5], the car-following models [6–21], the gas kinetic models [22–24] and so on [25–38].

Bando [39] firstly put forward the car-following model, it was depended on the consideration that each vehicle would adjust its own optimal velocity through the driving state of the vehicle in front. Then, Nagatani [40] presented the lattice model which was constructed by discretizing the model of Kerner [41]. What is more, because the lattice hydrodynamic model transforms the complex traffic system into the form of density wave for theoretical research, which makes it more intuitive to study the traffic flow. Subsequently, a large number of extended effects are considered, such as the backward looking effect [42–47], the effect of interruption [48,49], two-lane highway [50–56], optimal current difference effect [57–64] etc.

Moreover, roads in traffic network are always complex and changeable. Taking curved roads as an example, because the vehicles are subject to the centripetal force during driving on curved roads, more factors should be considered to reduce traffic congestion compared with straight roads. Based on Nagatani's model, Cao and Shi [65] put forward an improved lattice model on curved road, which mainly studied the influence of friction coefficient and the curvature radius on traffic flow. Because the driver's driving environment became irregular, it caused the change of traffic flow. In 2016, Zhou and

* Corresponding author at: Faculty of Maritime and Transportation, Ningbo University, Ningbo 315211, China.
E-mail address: gehongxia@nbu.edu.cn (H. Ge).

https://doi.org/10.1016/j.physa.2020.125023
0378-4371/

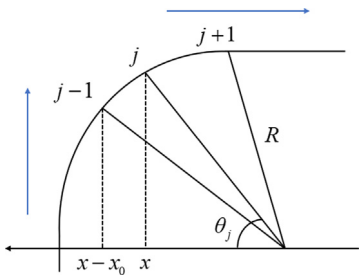

Fig. 1. The physical form of the model under curved road.

Shi [66] put forward a lattice hydrodynamic model, which considered the curved road. It verified that the factors of radian, friction coefficient and the curvature radius could stabilize the traffic flow. Jin et al. [67] carried out a lattice hydrodynamic model on curved road with passing. Actually, drivers are also a vital factor affecting traffic flow, to analyze the influence of it, a series of related researches are carried out. In 2017, Kaur and Sharma [68] presented a novel model considering driver's characteristics on a curved road. However, how driver's memory affects the optimal velocity is seldom studied in existing models. With the consideration of it, we come up with a novel lattice hydrodynamic model considering memory effect and the difference of optimal velocity on a curved road.

The structure of this article is designed as below: In Section 2, the extended model is formulated by considering memory effect and difference of optimal velocity on curved road. Section 3 deduced the stable condition for the new model. Then, the mKdV equation and its analytical solution are derived in Section 4. In Section 5, numerical simulations are carried out. Section 6 draws the conclusion.

2. The novel lattice hydrodynamic model

Nagatani [40] put forward the original lattice hydrodynamic model in 1998:

$$\partial_t \rho + \partial_x \rho v = 0 \tag{1}$$

$$\partial_t \rho v = a\rho_0 V(\rho(x+\delta)) - a\rho v \tag{2}$$

where ρ indicates density and v is velocity, ρ_0 means the average density.

Based on dimensionless, Eqs. (1) and (2) can be rewritten as below:

$$\partial_t \rho_j v_j = a\rho_0 V(\rho_{j+1}) - a\rho_j v_j \tag{3}$$

$$\partial_t \rho_j + \rho_0(\rho_j v_j - \rho_{j-1} v_{j-1}) = 0 \tag{4}$$

where $V(\cdot)$ is a monotonic decreasing function related to density on traffic system, which means the optimal velocity function. And it can be showed [69]:

$$V\left(\rho_j(t)\right) = \frac{V_{\max}}{2}\left[\tanh\left(\frac{2}{\rho_0} - \frac{\rho_j(t)}{\rho_0^2} - \frac{1}{\rho_c}\right) + \tanh\left(\frac{1}{\rho_c}\right)\right] \tag{5}$$

where ρ_c is the critical density.

Otherwise, Zhou and Shi [66] presented a modified model considering the bend effect. Fig. 1 shows the physical model of the curved road. The distance function on the curved road could be expressed as $y = \sqrt{R^2 - (x-R)^2}$, where R is the radius. l is the distance between the lattices j and $j-1$, which can be expressed as below:

$$l = \int_{x-x_0}^{x} \sqrt{1+y'^2}dx = \frac{x_0}{\sin\theta_j} \tag{6}$$

where θ_j indicates the angle at site j.

Therefore, the original lattice hydrodynamic model can be expressed by considering the effect of curved road:

$$\partial_t \rho_j + \frac{\rho_0}{\sin\theta_j}\left(\rho_j v_j - \rho_{j-1} v_{j-1}\right) = 0 \tag{7}$$

$$\partial_t \rho_j v_j = \frac{a\rho_0}{\sin\theta_j} V\left(\rho_{j+1}\right) - a\rho_j v_j \tag{8}$$

Also, the modified optimal velocity function changes on curved road [69], it can be showed as:

$$V\left(\rho_j(t)\right) = k\frac{\sqrt{\mu g R}}{2}\left\{\tanh\left[\frac{2}{\rho_0} - \frac{\rho_j(t)}{\rho_0^2} - \frac{1}{\rho_c}\right] + \tanh\left(\frac{1}{\rho_c}\right)\right\} \tag{9}$$

where $V_{\max} = \sqrt{\mu g R}$ is the maximal velocity on curved road, k expresses a control over $V_{\max}$, μ is the friction coefficient of the bend, g is gravitational acceleration.

As the traffic flow can be affected with many different factors, such as the factor of driver's behavior. Because different drivers will adjust the velocity of their vehicular according to their behavior. Therefore, drivers' adjustment of expected density is also changed. And, the value of optimal velocity will be changed by driver's behavior. In the case of driver's memory effect and the difference of optimal velocity, the extended lattice hydrodynamic model on curved road could be obtained:

$$\partial_t \rho_j(t)\, v_j(t) = \frac{a\rho_0}{\sin\theta_j} V\left(\rho_{j+1}(t-\alpha\tau_0)\right) - a\rho_j(t)\, v_j(t) + \frac{a\rho_0\beta}{\sin\theta_j}\left[V\left(\rho_{j+2}(t-\alpha\tau_0)\right) - V\left(\rho_{j+1}(t-\alpha\tau_0)\right)\right] \tag{10}$$

$$\partial_t \rho_j + \frac{\rho_0}{\sin\theta_j}\left(\rho_j v_j - \rho_{j-1} v_{j-1}\right) = 0 \tag{11}$$

where $\frac{\rho_0}{\sin\theta_j}$ is the modified average density compared with straight, which accounting for the angle of bend. α means the parameter of driver's memory effect on time. β is the corresponding coefficient. τ_0 is driver's reaction time for driver's memory.

Combing Eqs. (10) with (11) by eliminating the process of v_j, we can determine the following model:

$$\partial_t^2 \rho_j(t) + a\partial_t \rho_j(t) + \frac{a\rho_0^2}{\sin^2\theta_j}\left[V\left(\rho_{j+1}(t-\alpha\tau_0)\right) - V\left(\rho_j(t-\alpha\tau_0)\right)\right] + \frac{a\rho_0^2\beta}{\sin^2\theta_j}\left[V\left(\rho_{j+2}(t-\alpha\tau_0)\right) - 2V\left(\rho_{j+1}(t-\alpha\tau_0)\right) + V\left(\rho_j(t-\alpha\tau_0)\right)\right] = 0 \tag{12}$$

3. Linear analysis

By applying linear analysis, the memory effect and difference of optimal velocity on curved road is investigated. The uniform traffic flow means that the density and the optimal velocity are both constant values, which are chosen as ρ_0 and $V(\rho_0)$, respectively. The steady-state solution for model (12) is:

$$\rho_j(t) = \rho_0,\ v_j(t) = V(\rho_0) \tag{13}$$

A small deviation $y_j(t)$ is imposed on the steady state solution, which is expressed as below:

$$\rho_j(t) = \rho_0 + y_j(t) \tag{14}$$

Inserting (13) and (14) into (12), the following equation can be obtained:

$$\partial_t^2 y_j(t) + a\partial_t y_j(t) + \frac{a\rho_0^2}{\sin^2\theta_j} V'(\rho_0)\left[y_{j+1}(t) - y_j(t) - \alpha\tau_0\left(\partial_t y_{j+1}(t) - \partial_t y_j(t)\right)\right] + \frac{a\rho_0^2\beta}{\sin^2\theta_j} V'(\rho_0)\left[y_{j+2}(t) - 2y_{j+1}(t) + y_j(t) - \alpha\tau_0\left(\partial_t y_{j+2}(t) - 2\partial_t y_{j+1}(t) + \partial_t y_j(t)\right)\right] = 0 \tag{15}$$

where $V'(\rho_0) = \frac{\partial V(\rho)}{\partial \rho}|\rho = \rho_0$.

Determining the perturbation as $y_j = \exp(ikj + zt)$ and inserting it into (15), which results:

$$z^2 + az + \frac{a\rho_0^2}{\sin^2\theta_j} V'(\rho_0)\left[e^{ik} - 1 - \alpha\tau_0\left(ze^{ik} - z\right)\right] + \frac{a\rho_0^2\beta}{\sin^2\theta_j} V'(\rho_0)\left[e^{2ik} - 2e^{ik} + 1 - \alpha\tau_0\left(ze^{2ik} - 2ze^{ik} + z\right)\right] = 0 \tag{16}$$

By taking $z = z_1(ik) + z_2(ik)^2 + \cdots$ and substituting it into (16), the coefficients of (ik) and $(ik)^2$ can be obtained:

$$z_1 = -\frac{\rho_0^2 V'(\rho_0)}{\sin^2\theta_j} \tag{17}$$

$$z_2 = -\frac{\rho_0^4 V'^2(\rho_0)}{a\sin^4\theta_j} - \frac{\rho_0^4 V'^2(\rho_0)\alpha\tau_0}{2\sin^4\theta_j} - (1+2\beta)\frac{\rho_0^2 V'(\rho_0)}{2\sin^2\theta_j} \tag{18}$$

The small perturbation will not dissipate when $z_2 < 0$. On the contrary, it will disappear after a long time when $z_2 > 0$. Therefore, the neutral stability condition is:

$$a = -\frac{2\rho_0^2 V'(\rho_0)}{(1+2\beta)\sin^2\theta_j + \alpha\tau_0\rho_0^2 V'(\rho_0)} \tag{19}$$

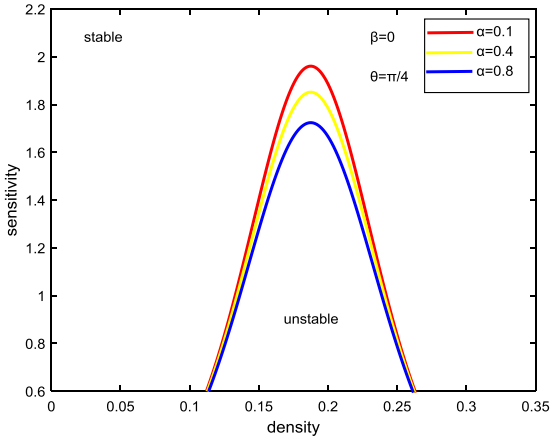

Fig. 2. The neutral stability curves for $\alpha = 0.1, 0.4, 0.8$ with $\beta = 0, \theta = \frac{\pi}{4}$.

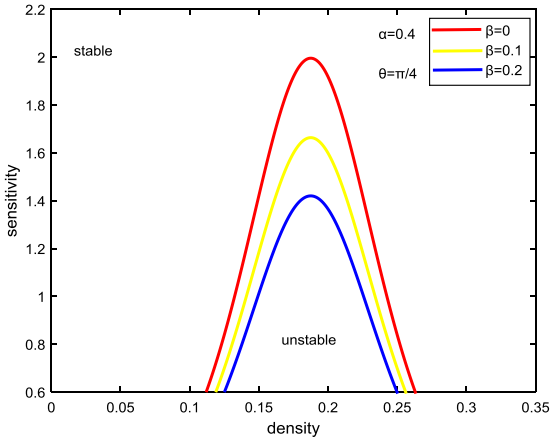

Fig. 3. The neutral stability curves for $\beta = 0, 0.1, 0.2$ with $\alpha = 0.4, \theta = \frac{\pi}{4}$.

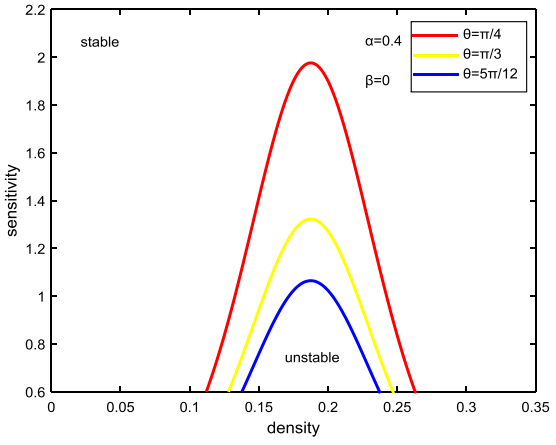

Fig. 4. The neutral stability curves for $\theta = \frac{\pi}{4}, \frac{\pi}{3}, \frac{5\pi}{12}$ with $\alpha = 0.4, \beta = 0$.

Thus, the stable condition is:

$$a > -\frac{2\rho_0^2 V'(\rho_0)}{(1+2\beta)\sin^2\theta_j + \alpha\tau_0\rho_0^2 V'(\rho_0)} \tag{20}$$

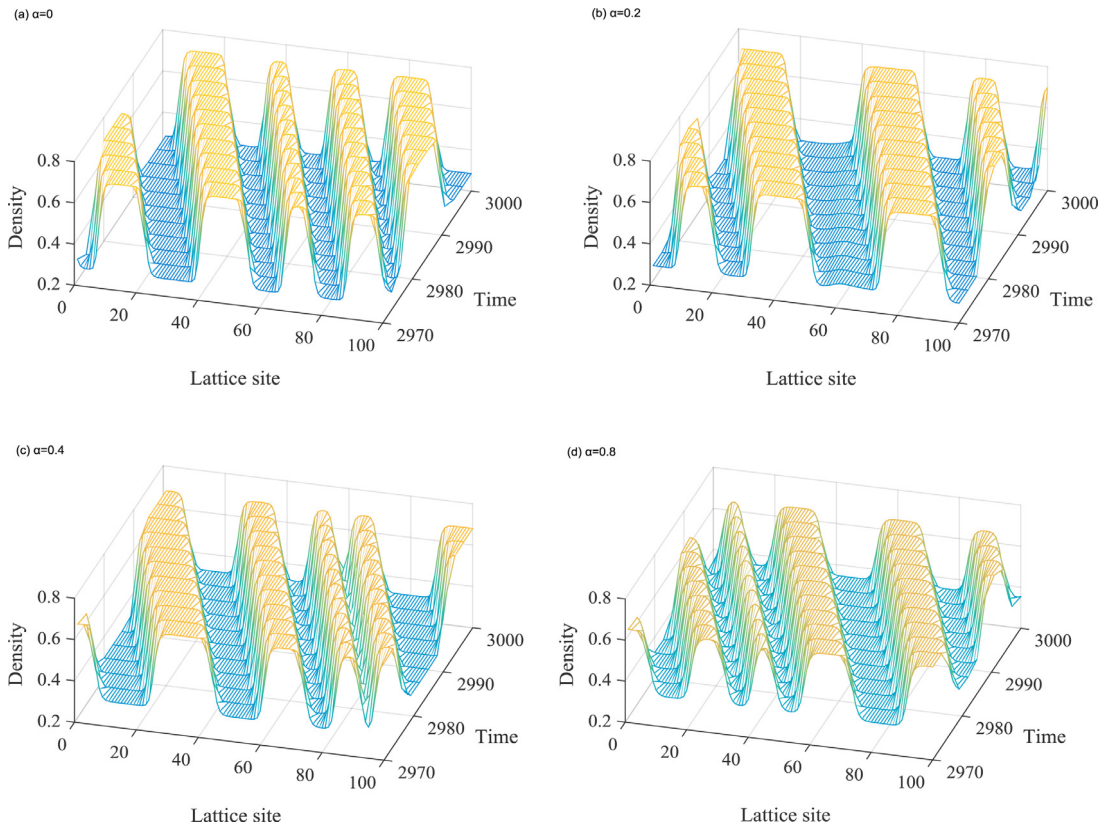

Fig. 5. The phase diagram of the model with $\alpha = 0, 0.2, 0.4, 0.8$.

When $\alpha = 0$ and $\beta = 0$, the stability criterion of the novel model is same as the model discussed by Zhou and Shi [66]. According to the (19), it is not difficult to find that effect of driver's memory and the difference of optimal velocity on curved road can help alleviate traffic congestion.

Figs. 2–4 show the neutral stability curves under different values of α, β and θ_j in the phase (ρ, a), respectively. In Fig. 2, we can clearly see the expansion of the stable region when we increase the value of α from 0.1 to 0.8. That is to say, considering driver's memory effect can effectively improve the overall stability of the traffic system. In Fig. 3, it shows the variation trend of the neutral stability curves when $\beta = 0, 0.1, 0.2$, respectively. From the phenomenon that the vertex decreases obviously while increasing β, it can be judged that the difference of optimal velocity effect is beneficial for traffic flow. There are the neutral stability curves in Fig. 4, which correspond to $\theta_j = \frac{\pi}{4}, \frac{\pi}{3}, \frac{5\pi}{12}$, respectively. Moreover, the analysis of curved road becomes indistinguishable from straight ones for $\theta_j = \frac{\pi}{2}$, and the stable region can be achieved in the maximum state.

4. Nonlinear analysis

Nonlinear analysis is presented near (ρ_c, a_c) to derive the mKdV equation. For $0 < \varepsilon \ll 1$, the slow variables X and Y are taken as:

$$X = \varepsilon(j + bt), T = \varepsilon^3 t \tag{21}$$

where b is a constant to be determined.

The expression for $\rho_j(t)$ is showed in the equation:

$$\rho_j(t) = \rho_c + \varepsilon R(X, T) \tag{22}$$

After substituting (21) and (22) into (12), the method of Taylor is used to expand them to the fifth power of ε, and the expanded equation is as follows:

$$\varepsilon^2 k_1 \partial_X R + \varepsilon^3 k_2 \partial_X^2 R + \varepsilon^4 \left(\partial_T R + k_3 \partial_X^3 R + k_4 \partial_X R^3\right) + \varepsilon^5 \left(k_5 \partial_X \partial_T R + k_6 \partial_X^2 R^3 + k_7 \partial_X^4 R\right) = 0 \tag{23}$$

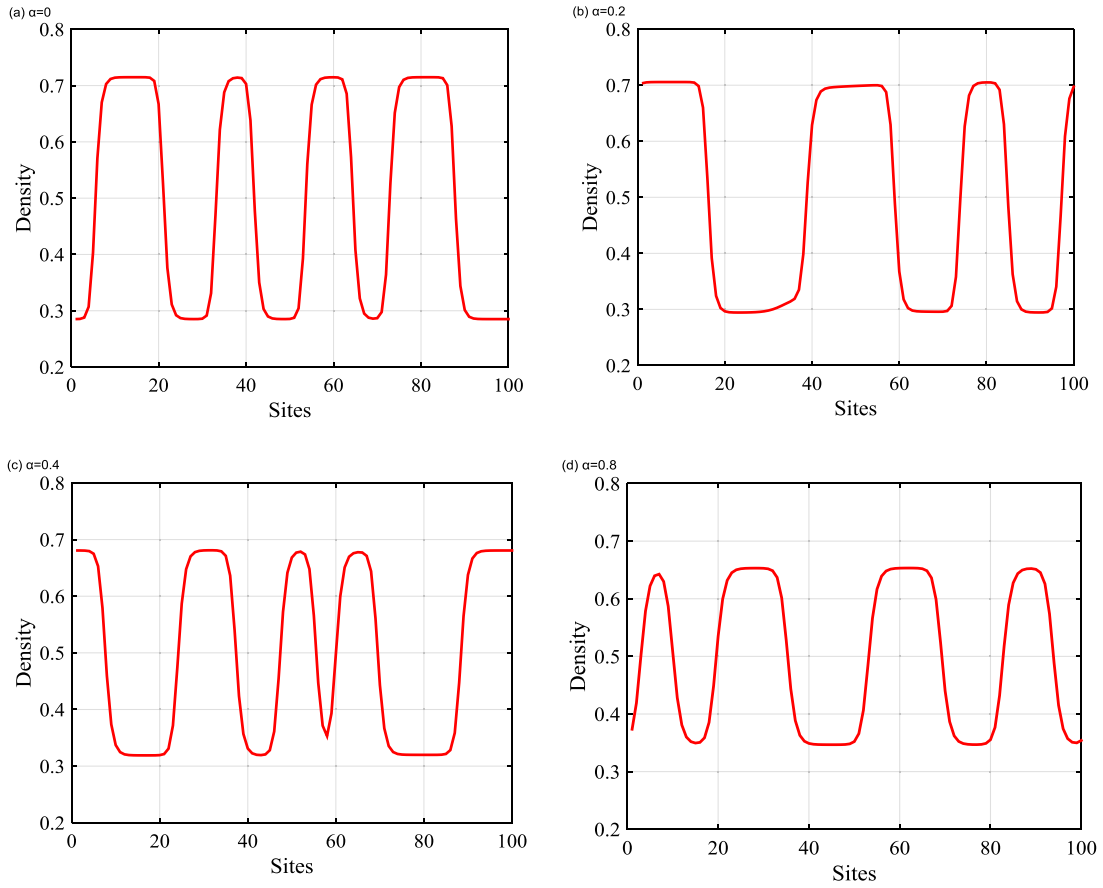

Fig. 6. The density profile at $t = 10\,300$ s corresponds to Fig. 5.

Table 1 shows the specific values of k_i $(i = 1, 2, 3 \ldots, 7)$. where $V' = \frac{\partial V(\rho)}{\partial \rho} |\rho = \rho_c$ and $V''' = \frac{\partial^3 V(\rho)}{\partial \rho^3} |\rho = \rho_c$. The value of a_c near (ρ_c, a_c) is as:

$$a_c = \left(1 + \varepsilon^2\right) a \tag{24}$$

In terms of $b = -\frac{\rho_0^2 V'}{\sin^2 \theta_j}$, the simplified equation is described as:

$$\varepsilon^4(-g_1 \partial_X^3 R + g_2 \partial_X R^3 + \partial_T R) + \varepsilon^5(g_4 \partial_X^4 R + g_5 \partial_X^3 R^3 + g_3 \partial_X^2 R) = 0 \tag{25}$$

where the coefficients g_i $(1, 2, \ldots, 5)$ are given in Table 2.

Let

$$T = \frac{1}{g_1} T', R = \sqrt{\frac{g_1}{g_2}} R' \tag{26}$$

Substituting Eq. (26) into Eq. (25), the mKdV equation with $O(\varepsilon)$ is derived as below:

$$\partial_{T'} R' = \partial_X^3 R' - \partial_X R'^3 + \varepsilon \left[\frac{g_3}{g_1} \partial_X^2 R' + \frac{g_4}{g_1} \partial_X^4 R' + \frac{g_5}{g_2} \partial_X^2 R'^3 \right] \tag{27}$$

So, the (27) could be simplified in the following form:

$$\partial_{T'} R' = \partial_X^3 R' - \partial_X R'^3 + \varepsilon M \left[R'\right] \tag{28}$$

where $M\left[R'\right] = \frac{g_3}{g_1} \partial_X^2 R' + \frac{g_4}{g_1} \partial_X^4 R' + \frac{g_5}{g_2} \partial_X^2 R'^3$.

Ignoring $O(\varepsilon)$, the kink–antikink solution of Eq. (28) is obtained:

$$R_0'\left(X, T'\right) = \sqrt{c} \tanh\left(\sqrt{\frac{c}{2}}\left(X - cT'\right)\right) \tag{29}$$

Table 1
The specific values of k_i for the model.

k_1	k_2
$b + \frac{\rho_c^2 V'}{\sin^2\theta_j}$	$\frac{b^2}{a} + \frac{\rho_c^2 V'}{2\sin^2\theta_j}(1 + 2\beta - 2\alpha\tau_0 b)$
k_3	k_4
$\frac{\rho_c^2 V'''(1+6\beta-9b\alpha\tau_0)}{6\sin^2\theta_j}$	$\frac{\rho_c^2 V'''}{6\sin^2\theta_j}$
k_5	k_6
$\frac{2b}{a} - \frac{\rho_c^2 V' b\alpha\tau_0}{\sin^2\theta_j}$	$\frac{\rho_c^2 V'(1+14\beta+20b\alpha\tau_0)}{24\sin^2\theta_j}$
k_7	
$\frac{\rho_c^2 V'''(1+2\beta)}{12\sin^2\theta_j}$	

Table 2
The specific values of g_i for the model.

g_1	g_2	g_3
$-\frac{\rho_c^2 V'(1+6\beta-9b\alpha\tau_0)}{6\sin^2\theta_j}$	$\frac{\rho_c^2 V'''}{6\sin^2\theta_j}$	$\frac{\alpha\tau_0\rho_c^4 V'^2}{24\sin^4\theta_j}$
g_4	g_5	
$\frac{\rho_c^2 V'(1+14\beta+20b\alpha\tau_0)}{24\sin^2\theta_j}$	$\frac{\rho_c^2 V'''(1+2\beta)}{12\sin^2\theta_j}$	

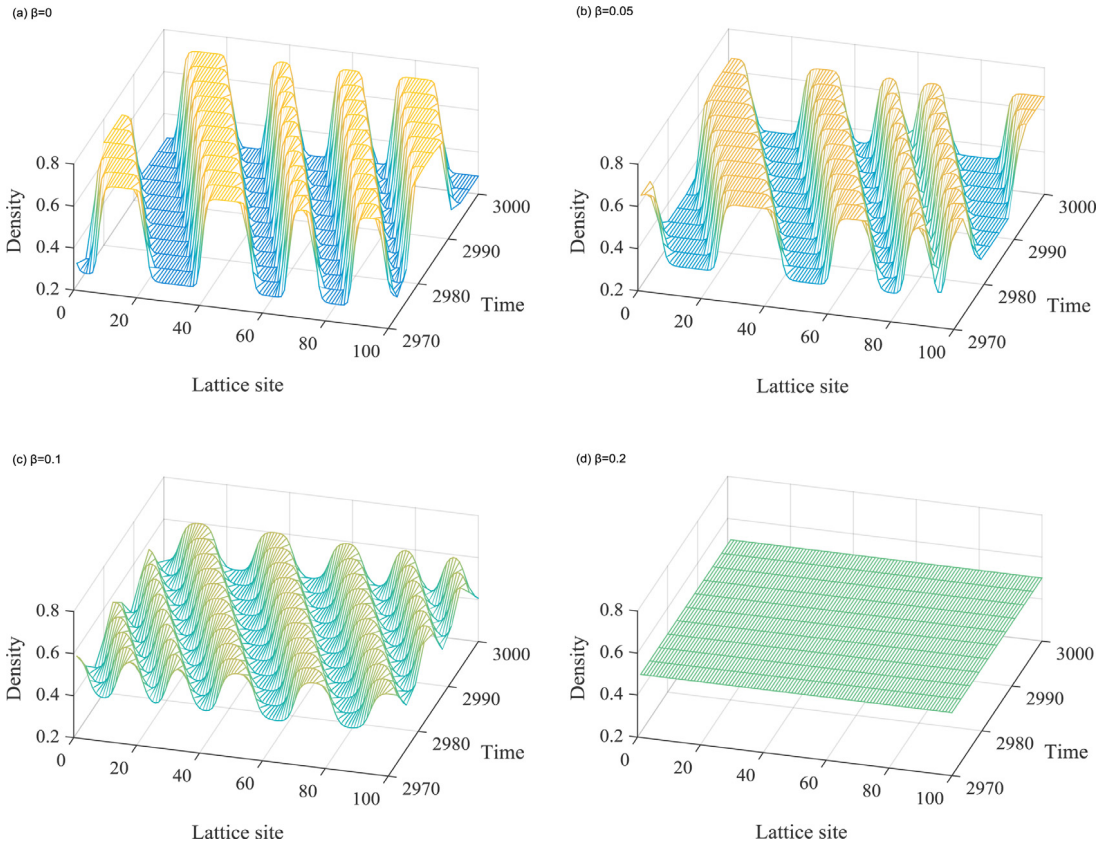

Fig. 7. The phase diagram of the model with $\beta = 0, 0.05, 0.1, 0.2$.

Let $R'(X,T') = R'_0(X,T') + \varepsilon R'_1(X,T')$, and the following solvability condition is applied to get the value of c:

$$\left(R'_0, M\left[R'_0\right]\right) \equiv \int_{-\infty}^{+\infty} dX' R'_0 M\left[R'_0\right] = 0 \tag{30}$$

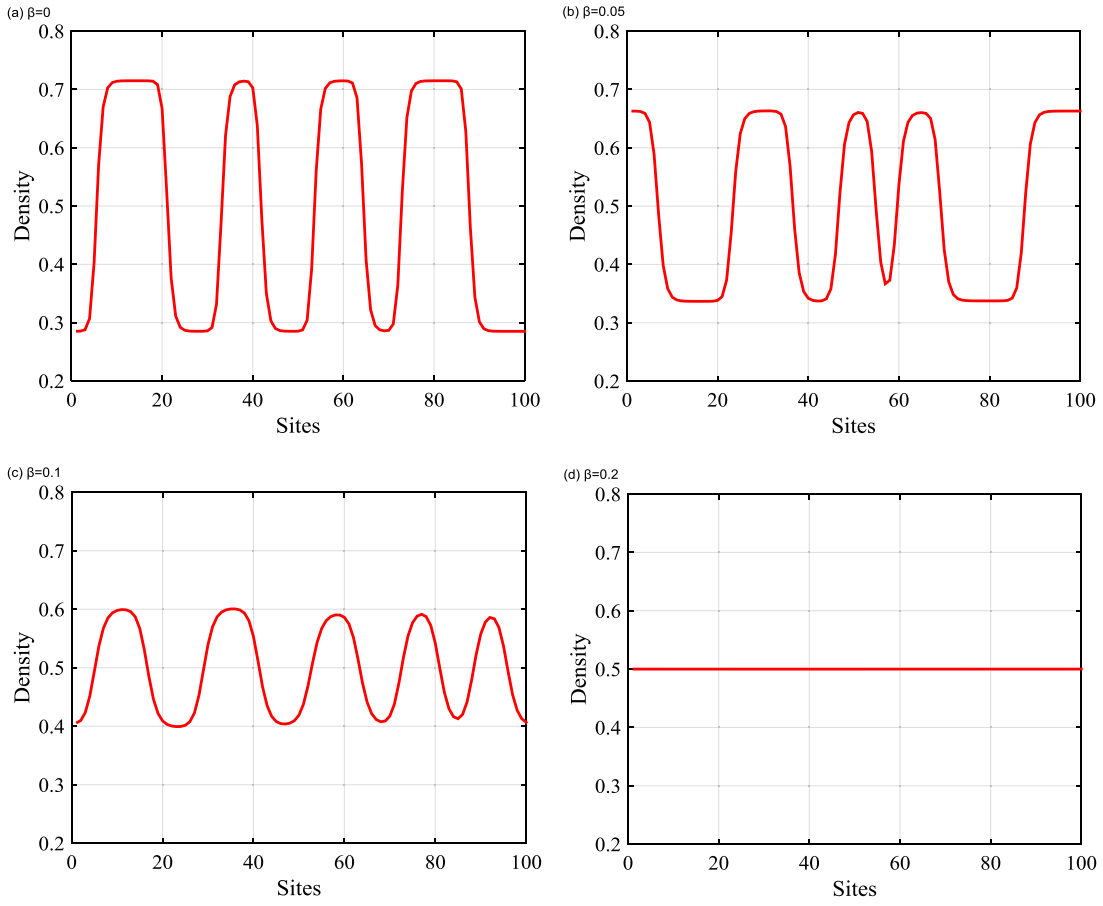

Fig. 8. The density profile at $t = 10\,300$ s corresponds to Fig. 7.

After solving the integral equation of (30), and $M\left[R_0'\right] = M\left[R\right]$ here. The value of c is evaluated as:

$$c = \frac{5g_2g_3}{2g_2g_4 - 3g_1g_5} \tag{31}$$

Whereafter, the soliton solution of the density can be rewritten when we substitute the variables into the original equation (22):

$$\rho_j\left(t\right) = \rho_c + \sqrt{\frac{g_1c}{g_2}\left(\frac{a_c}{a} - 1\right)} \times \tanh\sqrt{\frac{c}{2}\left(\frac{a_c}{a} - 1\right)} \times \left[j + \left(1 - cg_1\right)\left(\frac{a_c}{a} - 1\right)t\right] \tag{32}$$

In addition, the amplitude A of the density is:

$$A = \sqrt{\frac{g_1c}{g_2}\left(\frac{a_c}{a} - 1\right)} \tag{33}$$

With the nonlinear analysis above, the density wave of the mKdV equation changes with α, β and θ_j, which proves the effect of the new model on traffic system. In other words, when considering driver's memory effect, the difference of optimal velocity and curved road, the phenomenon of traffic jams can develop in a positive direction.

5. Numerical simulation

Numerical simulations are carried out to explore the impact of memory effect and difference of optimal velocity on traffic stability. The proposed novel lattice model of Eq. (12) is discretized through the difference scheme:

$$\rho_j\left(t + 2\Delta t\right) - 2\rho_j\left(t + \Delta t\right) + \rho_j\left(t\right) + a\Delta t\left[\rho_j\left(t + \Delta t\right) - \rho_j\left(t\right)\right]$$
$$+ \frac{a\rho_0^2\Delta t^2}{\sin^2\theta_j}\left[V\left(\rho_{j+1}\left(t - \alpha\tau_0\right)\right) - V\left(\rho_j\left(t - \alpha\tau_0\right)\right)\right] +$$

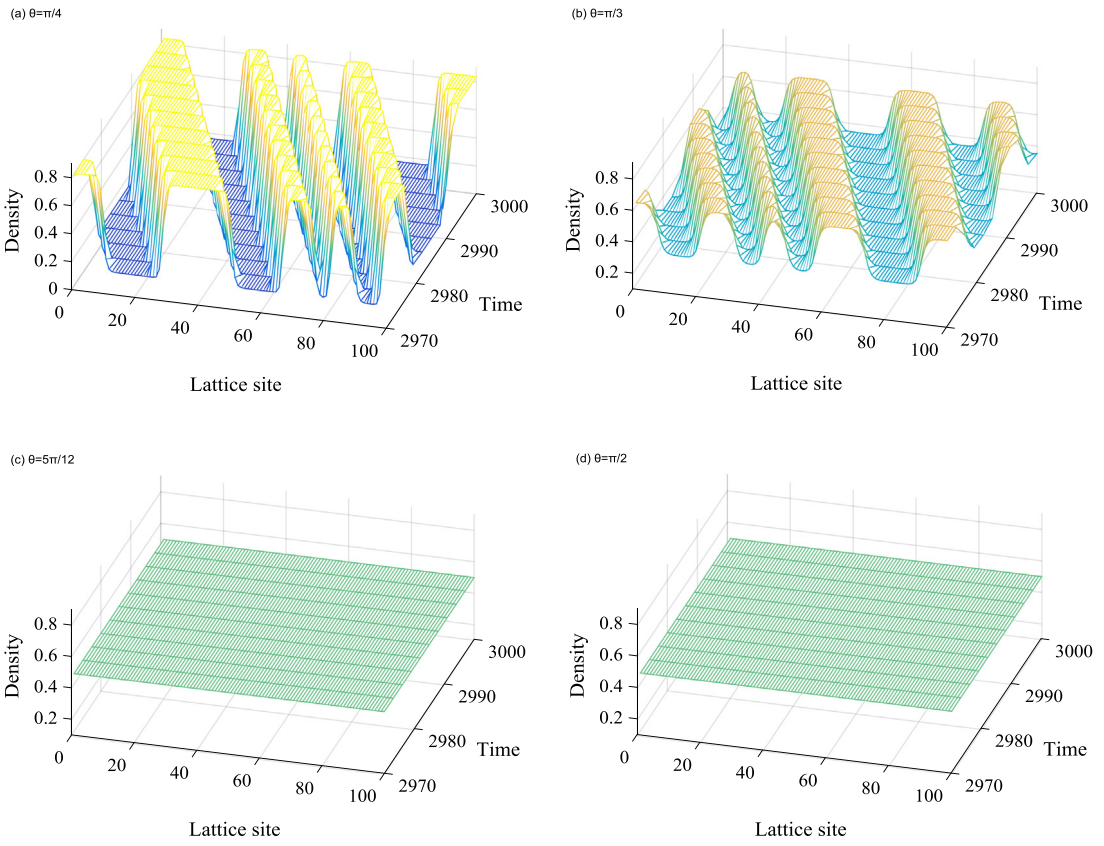

Fig. 9. The phase diagram of the model with $\theta_j = \frac{\pi}{6}, \frac{\pi}{3}, \frac{5\pi}{12}, \frac{\pi}{2}$.

$$\frac{a\rho_0^2\beta\Delta t^2}{\sin^2\theta_j}\left[V\left(\rho_{j+2}\left(t-\alpha\tau_0\right)\right)-2V\left(\rho_{j+1}\left(t-\alpha\tau_0\right)\right)+V\left(\rho_j\left(t-\alpha\tau_0\right)\right)\right]=0 \tag{34}$$

We can get the initial conditions:

$$\rho_j\left(1\right)=\rho_j(0)=\begin{cases}\rho_0, & j\neq\dfrac{N}{2},\dfrac{N}{2}+1,\\ \rho_0-0.05, & j=\dfrac{N}{2},\\ \rho_0+0.05, & j=\dfrac{N}{2}.\end{cases} \tag{35}$$

where $N=100$, $\rho_0=\rho_c=0.5$, $\mu=0.3$, $g=10$, $\tau_0=0.01$, $R=20$, $k=0.14$, $a=2.4$.

Fig. 5 shows the three-dimensional structure of the density wave curves, which are obtained for different α when $\beta=0, \theta_j=\pi/3$ by numerical simulation. From Fig. 5(a), the density curve fluctuates most strongly for $\alpha=0$, and traffic flow is disorganized. When we increase the value of α ($=0.4, 0.6, 0.8$), the fluctuation of density curve gradually becomes gentle with the increase of α. Therefore, it is obvious that memory effect plays a positive role in traffic flow.

In Fig. 6, the profile of density at time $t=10\,300$ s is indicated. When the value of α increases from 0 to 0.8, the amplitude of density waves decreases. It also demonstrated that memory effect can reduce traffic congestions.

Fig. 7 indicates the traffic patterns with different β when $\alpha=0.1, \theta_j=\pi/4$. For $\beta=0, 0.05, 0.1, 0.2$, the time evolution of density is exhibited, respectively. In patterns (a), (b) and (c), the kink–antikink density waves are showed by the lead of the initial disturbance, the change of the amplitude disturbance is drastic, it means traffic jams occur. Actually, the curve of amplitude disturbance evolves into a linear state in pattern (d). This means that under this condition, the parameter value reaches the stable condition, and the traffic flow will gradually become stable. We can determine that the difference of optimal velocity effect on curved road is significant to stabilize traffic flow.

Fig. 8 shows the density profile of the two-dimensional state at $t=10\,300$ s, which corresponds to Fig. 7. From the process of graphs evolution, we can see the specific change of a small disturbance on density. When increasing the value of β, the amplitudes of the density decreased. That is to say, traffic jams could be alleviated with the idea of difference of optimal velocity on curved road.

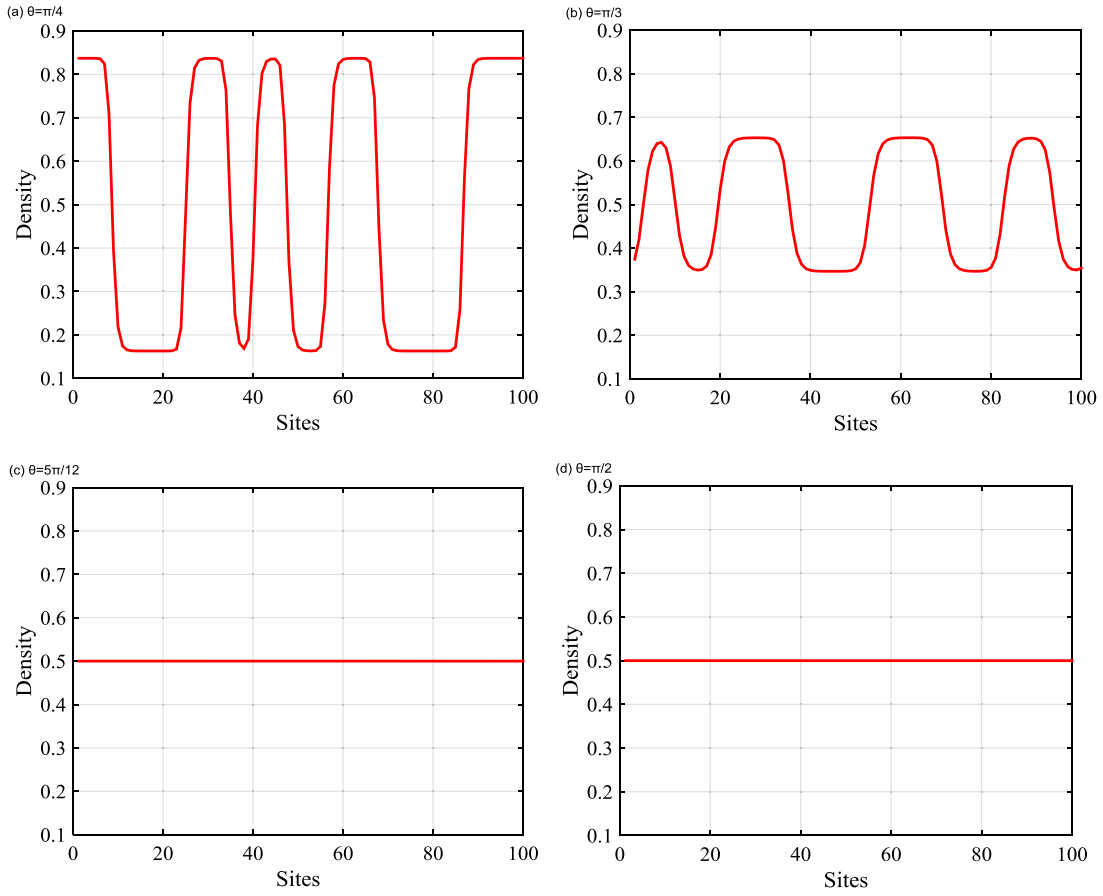

Fig. 10. The density profile at $t = 10\,300$ s corresponds to Fig. 9.

Fig. 9 shows the traffic patterns with different θ_j for $\alpha = 0.8$, $\beta = 0$, the kink–antikink density waves are exhibited. The conditions given in (a) and (b) do not satisfy the steady-state requirements, the small amplitude disturbance will develop into a congestion flow. From patterns (c) and (d), the density curves reach a stable state when $\theta = \frac{5\pi}{12}$ and $\frac{\pi}{2}$, it shows that under this condition, the traffic flow has met the requirement of its steady-state critical value. The results convey the message that within the value of range, with the increase of the angle of the curve, the phenomenon of traffic congestion continues to be improved until it reaches a stable state. It also means that the consideration of the angle of the curve has practical significance for traffic flow.

In Fig. 10, it shows the density curves variation in two-dimensional form at $t = 10\,300$ s. The larger the value of θ_j, the smaller the amplitude of density and finally reaches a stable state. The phenomenon of traffic jams could be alleviated when the factor of angle of curved road is taken into account.

6. Conclusion

A novel lattice hydrodynamic model which takes memory effect and the difference of optimal velocity on curved road into account is presented. Through linear analysis, the stability condition is obtained. Near the vertex of neutral stability curve, the mKdV equation is derived by applying nonlinear analysis. Numerical examples are performed to explored how these two factors infect traffic flow stability. Analytical results coincide well with numerical results. Both numerical and exact results demonstrate that memory effect and difference of optimal velocity play positive role in traffic stabilization.

CRediT authorship contribution statement

Qingying Wang: Conceptualization, Methodology. **Rongjun Cheng:** Data curation, Numerical simulation, Writing - original draft. **Hongxia Ge:** Supervision, Writing - review & editing.

Declaration of competing interest

The authors declare that they have no known competing financial interests or personal relationships that could have appeared to influence the work reported in this paper.

Acknowledgments

This work is supported by the Program of Humanities and Social Science of Education Ministry of China (Grant No. 20YJA630008) and the Natural Science Foundation of Zhejiang Province, China (Grant No. LY20G010004) and the National Key Research and Development Program of China-Traffic Modeling, Surveillance and Control with Connected & Automated Vehicles (Grant No. 2017YFE9134700) and the K.C. Wong Magna Fund in Ningbo University, China.

References

[1] M. Gerhardt, H. Schuster, J.J. Tyson, Science 247 (1990) 1563–1566.
[2] A.A. Patel, E.T. Gawlinski, S.K. Lemieux, R.A. Gatenby, J. Theoret. Biol. 213 (2001) 315–331.
[3] C.M. Almeida, J.M. Gleriani, E.F. Castejon, B.S. Soares, Int. J. Geogr. Inf. Sci 22 (2008) 943–963.
[4] S.G. Berjak, J.M. Hearne, Ecol. Model 148 (2002) 133–151.
[5] T.Q. Tang, Y.X. Rui, J. Zhang, H.Y. Shang, Physica A 492 (2018) 1782–1797.
[6] T.Q. Tang, Y.P. Wang, X.B. Yang, Y.H. Wu, Nonlinear Dyn. 70 (2012) 1397–1405.
[7] T.Q. Tang, C. Li, H. Huang, H. Shang, Nonlinear Dyn. 67 (2012) 437–443.
[8] D. Chen, D.H. Sun, M. Zhao, T. Zhou, S.L. Cheng, Physica A 502 (2018) 135–147.
[9] D.H. Sun, D. Chen, M. Zhao, W.M. Liu, L.J. Zheng, Physica A 501 (2018) 293–307.
[10] T. Wang, R.J. Cheng, H.X. Ge, IEEE Access 7 (2019) 174725–174733.
[11] Y. Rong, H.Y. Wen, Phys. Lett. A 382 (2018) 1341–1352.
[12] W.X. Zhu, H.M. Zhang, Physica A 496 (2017) 274–285.
[13] H.X. Ge, R.J. Cheng, Z.P. Li, Physica A 387 (2008) 5239–5245.
[14] H.X. Ge, R.J. Cheng, S.Q. Dai, Physica A 357 (2005) 466–476.
[15] W.X. Zhu, L.D. Zhang, Physica A 449 (2016) 265–274.
[16] W.X. Zhu, D.Z. Li, Physica A 492 (2018) 2154–2165.
[17] W.X. Zhu, D. Jun, L.D. Zhang, Commun. Nonlinear Sci. Numer. Simul. 39 (2016) 427–441.
[18] H. Ou, T.Q. Tang, Physica A 495 (2018) 260–268.
[19] T.Q. Tang, J. Zhang, K. Liu, Physica A 473 (2017) 45–52.
[20] Y.Q. Sun, H.X. Ge, R.J. Cheng, Physica A 521 (2019) 752–761.
[21] T. Wang, R.J. Cheng, H.X. Ge, Physica A 527 (2019) 121425.
[22] R. Atkinson, D.L. Baulch, R.A. Cox, R.F. Hampson, J.A. Kerr, M.J. Rossi, J. Troe, J. Phys. Chem. Ref. Data 26 (1997) 521–1011.
[23] M. Treiber, A. Hennecke, D. Helbing, Phys. Rev. E 59 (1999) 239–253.
[24] D. Helbing, A. Hennecke, V. Shvetsov, M. Treiber, Transp. Res. B 35 (2001) 183–211.
[25] T. Nagatani, Physica A 261 (1998) 599–607.
[26] D.H. Sun, G.H. Peng, Chin. Phys. B 18 (2009) 3724–3735.
[27] L. Yu, T. Li, Z.K. Shi, Phys. Lett. A 374 (2010) 2346–2355.
[28] A.K. Gupta, I. Dhiman, Internat. J. Modern Phys. C 25 (2014) 1450045.
[29] R.J. Cheng, H.X. Ge, J.F. Wang, Phys. Lett. A 381 (2017) 1302–1312.
[30] R.J. Cheng, H.X. Ge, J.F. Wang, Phys. Lett. A 381 (2017) 2608–2620.
[31] R.J. Cheng, H.X. Ge, J.F. Wang, Phys. Lett. A 381 (2017) 2792–2800.
[32] R.J. Cheng, H.X. Ge, J.F. Wang, Appl. Math. Comput. 332 (2018) 493–505.
[33] X. Wu, X.M. Zhao, H.S. Song, Q. Xin, S.W. Yu, Physica A 515 (2019) 192–198.
[34] R.J. Cheng, Y.N. Wang, Physica A 513 (2019) 510–517.
[35] C.T. Jiang, H.X. Ge, R.J. Cheng, Physica A 513 (2019) 465–467.
[36] Q.Y. Wang, H.X. Ge, Physica A 513 (2019) 438–446.
[37] N. Madaan, S. Sharma, Internat. J. Modern Phys. B 33 (2019) 1950248.
[38] D. Kaur, S. Sharma, Eur. Phys. J. B 93 (2020) 1–10.
[39] K. Bando, M. Hasebe, A. Nakayama, Phys. Rev. E 51 (1995) 1035–1042.
[40] T. Nagatani, Physica A 271 (1998) 599–607.
[41] B.S. Kerner, P. Konhauser, Phys. Rev. E 48 (1993) 2335–2338.
[42] H.X. Ge, H.B. Zhu, S.Q. Dai, Eur. Phys. J. B 54 (2006) 503–507.
[43] D.H. Sun, X.Y. Liao, G.H. Peng, Physica A 390 (2011) 631–635.
[44] W.X. Zhu, Commun. Theor. Phys. 50 (2008) 753–756.
[45] X.L. Li, Internat. J. Modern Phys. C 19 (2008) 1113–1127.
[46] P.G. Hou, H.W. Yu, C. Yan, J.Y. Hong, Chin. J. Phys 55 (2017) 2092–2099.
[47] C.T. Jiang, R.J. Cheng, H.X. Ge, Nonlinear Dyn. 91 (2018) 777–784.
[48] G. Zhang, H. Liu, Modern Phys. Lett. B 31 (2017) 1750317.
[49] D.H. Sun, G. Zhang, W.N. Liu, M. Zhao, S.L. Cheng, T. Zhou, Nonlinear Dyn. 86 (2016) 269–282.
[50] M. Rickert, K. Nagel, M. Schreckenberg, A. Latour, Physica A 231 (1996) 534–550.
[51] T. Nagatani, Physica A 265 (1999) 297–310.
[52] N. Nagel, D.E. Wolf, P. Wagner, P. Simon, Phys. Rev. E 58 (1998) 1425–1437.
[53] G.H. Peng, Commun. Nonlinear Sci. Numer. Simul. 18 (2013) 559–566.
[54] T.Q. Tang, X.F. Luo, J. Zhang, L. Chen, Physica A 490 (2018) 1377–1386.
[55] D. Kaur, S. Sharma, Physica A 539 (2020) 122913.
[56] R. Kaur, S. Sharma, Physica A 499 (2018) 110–120.
[57] P. Redhu, A.K. Gupta, Nonlinear Dyn. 78 (2014) 957–968.
[58] S. Sharma, Nonlinear Dyn. 81 (2015) 991–1003.

[59] A.K. Gupta, P. Redhu, Phys. Lett. A 377 (2013) 2027–2033.
[60] C. Tian, D.H. Sun, M. Zhang, Commun. Nonlinear Sci. Numer. Simul. 16 (2011) 4524–4529.
[61] C.X. Ma, W. Hao, R.C. He, X.Y. Jia, F.Q. Pan, J. Fan, R.Q. Xiong, PLoS One 13 (2018) e0193789.
[62] C.X. Ma, W, Hao, F.Q. Pan, W. Xiang, PLoS One 13 (2018) e0198931.
[63] C.X. Ma, R.C. He, W. Zhang, Path optimization of taxi carpooling, PLoS One 13 (2018) e0203221.
[64] Q.T. Zhai, H.X. Ge, R.J. Cheng, Physica A 490 (2018) 774–785.
[65] J.L. Cao, Z.K. Shi, Inter. J. Mod. Phys. C 26 (2015) 1550121.
[66] J. Zhou, Z.K. Shi, Nonlinear Dyn. 83 (2016) 1217–1236.
[67] Y.D. Jin, J. Zhou, Z.K. Shi, Nonlinear Dyn. 89 (2017) 107–124.
[68] R. Kaur, S. Sharma, Physica A 471 (2017) 59–67.
[69] T. Nagatani, Phys. Rev. E 59 (1999) 4857–4864.